Kinetics of an order-disorder phase transition with topological defects

Andrés M. Somoza,[1] Celeste Sagui,[2] and Christopher Roland[3]
[1]*Instituto de Ciencia de Materiales, Consejo Superior de Investigaciones Científicas, Madrid E-28049, Spain*
[2]*Department of Physics, McGill University, Montréal, Québec, Canada H3A 2T8*
[3]*Department of Physics, North Carolina State University, Raleigh, North Carolina 27695*
(Received 12 April 1996)

We have investigated the time evolution of a vectorial model *C* system following a temperature quench from the disordered state into the order-disorder coexistence region, with numerical Langevin simulations. The system is characterized by a vectorial, nonconserved order parameter coupled to a conserved quantity such as a concentration. Two different ordering mechanisms are observed. If the mean concentration c_o is $c_o > 1/2$, then the minority phase is the *ordered* phase and growth is driven by long-range diffusion. On the other hand, if $c_o < 1/2$, then it is the *disordered* phase that is in the minority. In this case, defects of the order parameter (vortices) are strongly coupled to that of the position of the disordered phase. Growth takes place primarily via the diffusion and coalescence of the defects, giving rise to an $n = 1/4$ growth exponent over a significant time regime. [S1063-651X(96)09911-4]

PACS number(s): 64.60.Cn, 05.70.Ln

I. INTRODUCTION

In recent years, there has been great interest in the dynamics of defects created during a symmetry-breaking phase transition [1]. Typically, an instability produces topological defects following a quench into the broken symmetry phase. The subsequent time evolution, or dynamics of ordering, is characterized by an annealing away of these defects [2,3]: the free energy of the system is reduced as the density of defects decreases. The nature of the order parameter, together with the conservation laws associated with it, determine the growth laws of the characteristic length scales of the system, as well as the associated scaling functions.

The growth laws and scaling function for systems characterized by a single order parameter have been, for the most part, determined and understood [3]. For example, for a system with a scalar, nonconserved order parameter (model *A* [4]), the relevant topological defects are the domain walls or interfaces separating the different ordered phases. The annealing away of these interfaces is driven by curvature, and the average domain size $R(t)$ obeys a power-law growth $R \sim t^n$ with growth exponent $n = 1/2$ [5]. If the system involves a scalar, conserved order parameter (model *B*), then growth takes place via the classical Lifshitz-Slyozov mechanism of long-ranged diffusion with growth exponent $n = 1/3$ [6].

However, more complicated phenomenology arises when the system is characterized by more than one order parameter. In such cases, defects of a more complex nature form, and the nature of the dynamics is changed significantly. The simplest of such cases arises when the system is characterized by both a scalar, nonconserved order parameter and a scalar, conserved quantity such as a concentration. This situation may describe, for instance, metal alloys in which the nonconserved order parameter is associated with the symmetry of the alloy [7]. When such a system is quenched into the order-disorder coexistence region of its phase diagram, two types of interfaces are formed and, for a given concentration, the ratio of the associated surface tensions determines the morphology [8].

In this paper, we investigate the interesting changes that arise in such a system, when the nature of the nonconserved order parameter changes from that of a *scalar*, to that of a *vector*. This change is important because systems with a vector order parameter generate a different type of defects, namely, vortices, which in this case are coupled to the domain walls generated by the concentration variable. As we shall discuss, this changes the dynamics of the system over a significant time regime. Such a simplified model should be relevant for a number of experimental systems. For instance, a mixture of isotropic fluids and two-dimensional nematics [9] and smectic-*C* liquid crystal thin films [10], constrained by surfaces so that the director is approximately planar may be adequately represented by this model. Wong *et al.* [9] have in fact studied the coarsening behavior of two lyotropic liquid-crystal systems that were quenched from the isotropic phase into either the nematic phase or a region of coexistence between nematic and isotropic phases. In the coexistence region, both in two and three dimensions, they observed Porod's power-law behavior for the structure factor: $S(q) \sim q^{-(d+1)}$ for large wave vectors q, where d is the dimension of the system. This has been understood in terms of the scattering from the domains walls. Other systems, where our model may apply, include thin films of He^3-He^4 mixtures, mixtures of ferro- and paramagnets, and mixtures of smectic-*A* and smectic-*C* liquid crystals. We also note that a similar model was used to investigate growth of polycrystalline material [11]. In the latter study, the vector field was used to model the orientation of the local lattice structure, and the concentration variable the local atomic composition.

The system we consider exhibits both a stable disordered and a stable continuously degenerate ordered phase [8]. Thus, the free-energy minimum corresponding to the high-temperature minimum is also a minimum after a quench into

the order-disorder coexistence region, so that only very large fluctuations in the vectorial order parameter could drive the system to the degenerate ordered state. However, if one allows for differences in an associated concentration field, or some other related quantity, then a spinodal region can be created and phase separation will take place following a temperature quench. A situation like this is described by a model *C* system [4], and is to be contrasted with that of a model *A* and *B* system, where the disordered minimum of the free energy becomes unstable after a quench. In that case, the system is driven towards the equilibrium ordered states, which have a reduced symmetry. In model *C* systems, the disordered state is still stable after a quench, but the coupling of the order parameter to a conserved quantity such as a concentration makes the disordered phase unstable in the associated spinodal region. Transitions to the ordered states therefore become allowed.

The high-temperature, disordered phase of a two-dimensional model *C* system with a vectorial order parameter has continuous SO(2) symmetry. Suppose that such a system is quenched into the ordered part of the phase diagram (i.e., below the λ line, but above the first-order coexistence lines), and that the coupling between the order parameter and concentration is very weak. Then, the continuous symmetry would be broken into the Z_1 symmetry and the system would behave like a planar, *XY* model. The typical topological defects of this system are vortices, i.e., pointlike disclinations with an integral winding number [12]. These systems have been studied in the interesting context of two-dimensional melting, where the mechanism driving the phase transition from disorder to order is the pairing, and annihilation, of individual vortices and a continuous transition takes the system to quasi-long-range order [13]. Recently, there has been a number of computational investigation of the *XY* model and other related systems [14–17]. The work by Pargellis, Green, and Yurke [14] includes an experimental realization of the planar *XY* system by means of a confined nematic liquid crystal. When the spins are allowed to relax via linear damping from an initial random configuration, the system is expected to anneal diffusively so that the squared correlation length is proportional to time; assuming randomly distributed defects, the expected defect decay exponent is $n=1$. However, as Yurke *et al.* [18] pointed out, due to the presence of frictional forces, there exist logarithmic corrections to these scaling laws.

In this paper, we shall show how the usual *XY* planar model scenario gets dramatically modified when one allows coexistence with a disordered phase, in the presence of a concentration variable, i.e., we will investigate quenches into the order-disorder region of the phase diagram. We show that there exists a parameter regime in which the defects of the order parameter (the vortices) couple strongly to the position of the disordered phase. This changes the dominant mechanism of ordering from that of long-range diffusion or Lifshitz-Slyozov growth to one of defect annihilation over a significant time regime.

A brief summary of the structure of the paper is as follows. Section II discusses the model and gives details of the simulations; in Sec. III, we present the results with an emphasis upon the droplet morphology created and their growth. Section IV is reserved for a summary and conclusions.

II. MODEL

We begin with the Ginzburg-Landau free energy [19]

$$F[\phi,\vec{\psi}]=\int d\mathbf{r}\left\{\frac{1}{2}l_{\psi}^{2}\left|\boldsymbol{\nabla}\vec{\psi}(\mathbf{r})\right|^{2}+\frac{1}{2}l_{\phi}^{2}[\boldsymbol{\nabla}\phi(\mathbf{r})]^{2}+f(\phi,\vec{\psi})\right\}, \tag{1}$$

where $|\boldsymbol{\nabla}\vec{\psi}|^2=\Sigma_{i=1}^{m}(\boldsymbol{\nabla}\psi_i)(\boldsymbol{\nabla}\psi_i)$ and $f(\phi,\vec{\psi})$ is the bulk free-energy density,

$$f(\phi,\vec{\psi})=\tfrac{1}{2}r|\vec{\psi}|^2+u|\vec{\psi}|^4+v|\vec{\psi}|^6+\tfrac{1}{2}\chi_n^{-1}\phi^2+\gamma\phi|\vec{\psi}|^2-\Delta\phi. \tag{2}$$

Here $\vec{\psi}$ is a vectorial, nonconserved order parameter with *m* components, ϕ is the coupled conserved concentration, and $r,u,v,\chi_n,\gamma,l_{\psi}$, and l_{ϕ} are system parameters with $(v,\chi_n,l_{\psi},l_{\phi}>0)$. Δ is the chemical potential related to the concentration. The phase diagram for this system is well known [19]. A mean field analysis reveals that the system has a line of first-order phase transitions at

$$\tilde{r}\equiv r+2\Delta\gamma\chi_n=0, \tag{3}$$

$$\tilde{u}\equiv u-\tfrac{1}{2}\gamma^2\chi_n>0. \tag{4}$$

This line ends in a tricritical point at $\tilde{r}=0,\tilde{u}=0$. There is also a line of second-order phase transitions at $\tilde{r}=\tilde{r}_0\equiv(\tilde{u}^2/2v)$ and $\tilde{u}<0$. We investigated the dynamics of this system following a temperature quench from the disordered phase $(\tilde{r}>0,\ \tilde{u}>0)$ into the coexistence region. The units of energy, concentration and order parameter of this model may all be rescaled to give a dimensionless free-energy density [8]

$$f(c,\mathbf{y})=|\mathbf{y}|^2(1-|\mathbf{y}|^2)^2+\alpha(c+|\mathbf{y}|^2-1)^2+\frac{l_c^2}{2}(\boldsymbol{\nabla}c)^2+\frac{l_y^2}{2}|\boldsymbol{\nabla}\mathbf{y}|^2. \tag{5}$$

Here $\mathbf{y}$ and c are the rescaled vectorial order parameter and concentration, respectively. The model is given in terms of three positive constants: α, l_c, and l_y. We fix $\alpha=4$ and select the unit of length such that $l_c l_y=1$, but allow for variations in l_y. The local free energy is a three-dimensional function with coexisting minima in $(c,|\mathbf{y}|)=(1,0)$ (the disordered phase) and $(c,|\mathbf{y}|)=(0,1)$ (a continuously degenerate ordered phase).

The dynamics of the phase separation process is described by the coupled Langevin equations

$$\frac{\partial c}{\partial t}=\Gamma_c\nabla^2\left[\frac{\partial f(c,\mathbf{y})}{\partial c}-l_c^2\nabla^2 c\right]+\xi_c, \tag{6}$$

$$\frac{\partial \mathbf{y}}{\partial t}=-\Gamma_y\left[\frac{\partial f(c,\mathbf{y})}{\partial \mathbf{y}}-l_y^2\nabla^2\mathbf{y}\right]+\xi_y, \tag{7}$$

where ξ_c and ξ_y are stochastic variables obeying the fluctuation-dissipation relation. In this study, we neglect the thermal noise [20] and set the mobilities $\Gamma_c=\Gamma_y=1$.

The Langevin equations were solved numerically using Euler's method on two-dimensional grids of linear size $L=1024$ and 512, with periodic boundary conditions. The spatial mesh size and integration time step were chosen to be $\Delta x=1.0$ and $\Delta t=0.01$, respectively. Further reduction of these sizes did not change the solutions in any significant way. While systems of different sizes were simulated, most of our results were obtained for systems of length $L=512$, which displayed good self-averaging properties. The initial values of each component of **y** were chosen from a Gaussian distribution of zero mean and a second moment of 0.1, while the initial values of the c's were specified by a similar Gaussian distribution, but centered about the value c_o. To probe the different morphologies, single runs were carried out for $c_0=1/3$ and 2/3, and $l_y=0.8$, 1, 2, and 4. At least five independent runs were performed for each of the sets of parameters: $c_0=1/3$, $l_y=1$; and $c_0=1/3$, $l_y=4$.

For each simulation, we computed the pair correlation functions for both the conserved variable c and the nonconserved order parameter **y**. These are, respectively, defined as $C_c(\mathbf{r},t)=\langle[c(0,t)-c_0][c(\mathbf{r},t)-c_0]\rangle$ and $C_y(\mathbf{r},t)=\langle\mathbf{y}(0,t)\cdot\mathbf{y}(\mathbf{r},t)\rangle$, where the angle brackets indicate an ensemble average. With the circularly averaged values of these correlation functions, we were able to calculate two typical length scales $R_c(t)$ and $R_y(t)$ associated with each of the variables: $R_c(t)$ was defined as the first zero of the pair correlation function $C_c(r,t)$, and $R_y(t)$ as the value of r for which $C_y(t)$ takes on half of its value at the origin in the scaling regime. Two other distances obtained from the correlation functions are $L_c(t)=1/[1-C_c(0,t)/C_o]$, where $C_o=c_0(1-c_0)$ is the theoretical value of $C_c(0,t)$ in the scaling regime; and $L_y(t)=-1/[1-C_y(0,t)/Y_o]$, with $Y_o=1-c_0$. These distances are similar to the inverse perimeter densities used in other simulation studies as a measure of the average domain size. Other quantities computed include the mean radius, the radius of gyration, and the topological charge of each domain.

III. RESULTS AND DISCUSSION

A. Morphology

In this section, we discuss the role of the continuous symmetry of the ordered phase on the domain morphology. To better understand the phenomenology associated with a vectorial model C, we first review the scalar model C and the planar XY model, concentrating on the relevant physical features in these systems that contribute to the morphology of the vectorial model C.

We begin by discussing the results of the scalar model C (see, for example, [8] and references therein). In this case, the ordered phase corresponds to $c=0$, $y=\pm1$, and the disordered phase to $c=1$, $y=0$. It is now well established that the morphology depends upon whether the minority phase is ordered or disordered, as well as on the wetting properties of the interfaces. For $c_0>1/2$, the minority phase is ordered and forms isolated droplets. The order parameter inside each of these isolated droplets can take on either a positive or negative value, irrespective of the value inside other domains. In this case, the degeneracy of the ordered state does not play a qualitatively important role in the ordering process. Similarly, changes in the wetting properties of the interfaces are also not dramatic. A completely different situation arises when the minority phase is the disordered one ($c_0<1/2$). In this case, an ordered domain can grow to an infinite size, percolating throughout the system. Long-range order is not achieved, and order-order interfaces can persist in the system, even at very late times. The morphology itself depends upon the wetting properties of the interfaces in important ways. In the complete wetting regime ($l_y>0.79$), two ordered domains having different signs in the order parameter are separated by a macroscopic, disordered wetting layer. The disordered domains tend to surround the ordered domains and percolate throughout the system. Their morphology corresponds to that of elongated stripes with a few shrinking droplets, instead of a droplet morphology. In the partial drying regime ($l_y<0.60$), an ordered domain prefers to be in contact with another ordered domain, instead of a disordered one. The disordered domains therefore no longer surround the ordered domains, and therefore adopt a more compact shape. The intermediate case ($0.6<l_y<0.79$) corresponds to the partial wetting regime.

For the vectorial model C, the situation is different. As in the planar XY model, the director **y** may be thought of as representing a two-dimensional magnetization vector (or a polar molecule). The vectorial character of the order parameter precludes the existence of order-order interfaces so that the wetting properties characteristic of the interfaces in the scalar model C system will not be relevant. Instead, after a temperature quench, topological defects with an integral winding number are generated in the ordered phase.

To understand the phenomenology associated with this system, we briefly discuss the planar XY model and the scalar model C system. In the planar XY model [O(2) σ model], one can choose the director **y** such that $|\mathbf{y}|=1$ (say, $y_x=\cos\phi$ and $y_y=\sin\phi$). The free-energy density becomes $f(\phi)=(l_y^2/2)|\nabla\mathbf{y}|^2=(l_y^2/2)(\nabla\phi)^2$. The equilibrium equation $\delta F(\phi)/\delta\phi=0$ leads to $\nabla^2\phi=0$, so that the simplest nontrivial solution independent of $r=\sqrt{x^2+y^2}$ is

$$\phi=s\tan^{-1}\left(\frac{y}{x}\right)+c, \tag{8}$$

where $s=\pm1,\pm2,\pm3\ldots$ and $0\leqslant c<2\pi$. If we follow a path around the center, the director orientation ϕ changes by $2\pi s$. The integer number s is the *strength* of the disclination, i.e., the topological charge of the vortex. The energy of an isolated defect in a circular region of radius L is then

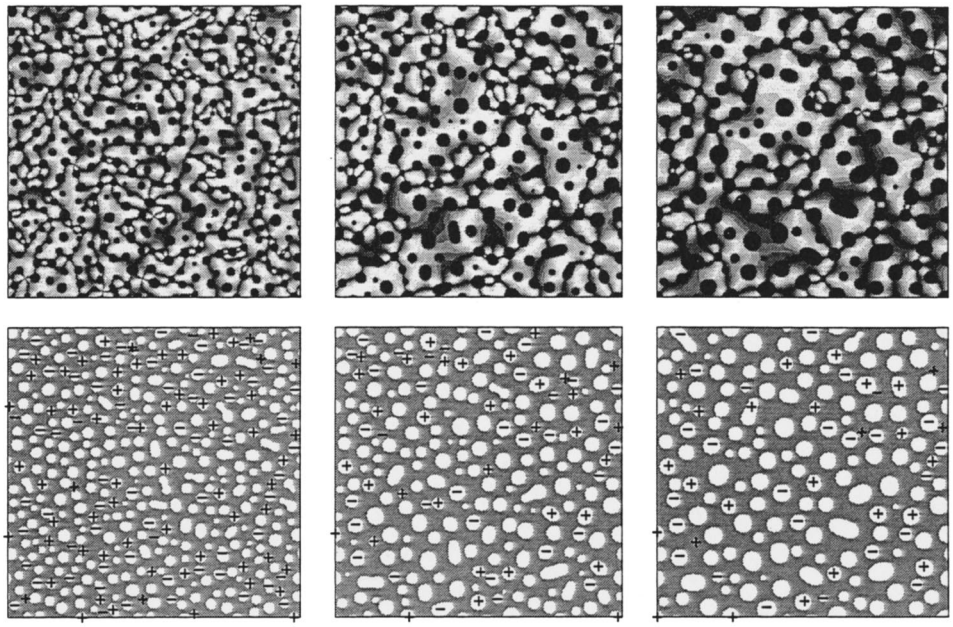

FIG. 1. Time evolution of the system for $c_0=1/3$ and $l_y=1$. From left to right, times correspond to $t=500$, 1500, and 2500. Top panel: schlieren textures. The gray scale is proportional to $|\mathbf{y}|^2\sin^2(2\phi)$. Bottom panel: Corresponding disordered domain morphology indicating the sign of the charged domains.

$$E=\int\int f(\phi)dxdy=\frac{l_y^2}{2}\int_0^{2\pi}d\theta\int_{r_c}^{L}rdr\,\frac{s^2}{r^2}$$

$$=\pi l_y^2 s^2\ln\left(\frac{L}{r_c}\right)+E_c, \tag{9}$$

where E_c is the core energy of the defect and r_c is the cutoff radius around the defect. The energy density (sometimes called ''elastic'' or ''topological'' energy) falls off like s^2/r^2, except inside the core. The total energy diverges logarithmically with the distance L, indicating that an isolated defect in an infinite plane has infinite energy. However, this situation does not arise, because the energy remains finite in the presence of defects of opposite charge. The interaction between two defects can be derived by substituting the solutions (8), centered at two different points, into the expression for the energy:

$$E=\pi l_y^2(s_1+s_2)^2\ln\left(\frac{L}{r_c}\right)-2\pi l_y^2 s_1 s_2\ln\left(\frac{r_{12}}{2r_c}\right), \tag{10}$$

with $r_c\ll r_{12}\ll L$. If $(s_1+s_2)=0$, the energy becomes independent of L. The effective force between defects is $2\pi l_y^2 s_1 s_2/r_{12}$ and is clearly long ranged. Note that while defects of equal sign repel, defects of opposite sign attract each other.

Convenient representations of the vectorial nature of the order parameter can be obtained by plotting the familiar ''Schlieren textures,'' such as shown in the top panels of Fig. 1, for a vectorial model C system with $c_0=1/3$. Such pictures are typically obtained by placing thin liquid-crystal films between two crossed polarizers. Apart from the dark spots, which correspond to domains of the disordered phase, there are bright and dark regions. In the black brushes, the director is either parallel or perpendicular to the plane of polarization of the incident light. The polarization is thus unchanged in these regions and consequently light is not transmitted by the cross analyzer. The black brushes originating from the points correspond to line singularities perpendicular to the film, or to point singularities in the two-dimensional case. The strength of a defect is defined as $s=1/4$ (number of brushes). The points that have four brushes correspond to point disclinations with charge ±1 (vortices), and are mostly centered in domains of the disordered phase ($c=1$ and $|\mathbf{y}|=0$), shown as black droplets in the schlieren textures. In analogy to the liquid-crystal system, the isotropic phase does not change the polarization. However, unlike the nematic case, the droplets with two brushes in our configurations have no topological charge. This is because the absence of the ''head-tail'' asymmetry, that characterizes the director of a nematic, does not allow for defects with $\pm(1/2)$ charge. The lower panels of Fig. 1 show the corresponding droplet morphology, indicating explicitly the charge of the domains.

We now discuss the role of the concentration on the domain morphology of the vector model C system. For $c_0>1/2$, it is the minority phase that is ordered. As in the case of the scalar model C system, it forms isolated droplets. The interior of these droplets is without defects, so that that vectorial nature of the order parameter does not play a role. However, its existence accounts for differences in the domain shapes with respect to the scalar model C or the model B systems, especially at early times. As Fig. 2 shows, the domains are not quite circular but elongated and curved, and sometimes branched. As time evolves, the elongation and branching disappears and the domains become more circular. Thus the late time regime is very similar to that of a model B system. Separated domains only interact through long-range diffusion, and remain unaware of the orientation of the order parameter inside each droplet.

We now turn to the case where $c_0<1/2$, where the minority phase is the disordered phase. Typical configurations are shown in Fig. 1. The continuous symmetry of the ordered phase completely changes the morphology with respect to the one obtained for the scalar order parameter. The absence of order-order interfaces precludes the stripe shape for the disordered domains, which now are droplets, as in the case

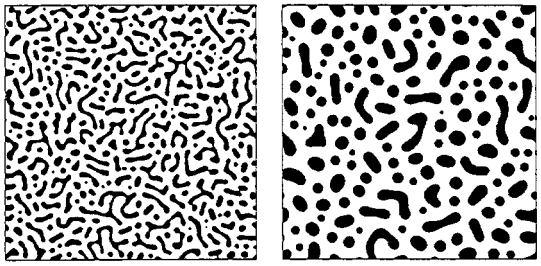

FIG. 2. Evolution of the concentration domains for $c_0=2/3$ and $l_y=1$. The black domains represent ordered phase while the white matrix represents disordered phase. The left configuration corresponds to $t=100$ and the right one to $t=800$.

with $c_0>1/2$. Inside the disordered domains $|\mathbf{y}|=0$ and thus there is no elastic or topological energy. Since the vicinity of a vortex is characterized by a large elastic energy density, the free energy of the system is minimized if a disordered domain sits on top of a vortex. In this way, the location of the vortices becomes coupled to the location of the concentration droplets (with $c=1$). Although not all the concentration domains have vortices (i.e., there are ''neutral'' domains), all the vortices are inside concentration domains (''charged'' domains). For an isolated defect with a disordered domain of radius R at the center, the energy E up to a distance L from the domain is

$$E=\pi l_y^2 s^2 \ln\left(\frac{L}{R}\right)+2\pi R\sigma-\pi R^2\Delta+E_c, \tag{11}$$

where σ is the surface tension (assumed independent of the orientation of $\mathbf{y}$) and Δ is the supersaturation of the system. In the expression above, the first term corresponds to the elastic energy, the second term is the surface energy of the domain and the third term is the volume free energy (here we assume small Δ). Thus the equilibrium equation $\partial E/\partial R=0$ gives the following solutions:

$$R_A=\frac{\sigma+\sqrt{\sigma^2-2l_y^2s^2\Delta}}{2\Delta}\sim\frac{\sigma}{\Delta}-\frac{l_y^2s^2}{2\sigma},$$

$$R_B=\frac{\sigma-\sqrt{\sigma^2-2l_y^2s^2\Delta}}{2\Delta}\sim\frac{l_y^2s^2}{2\sigma}-\frac{l_y^4s^4\Delta}{4\sigma^3}, \tag{12}$$

where the second equalities are valid for $\Delta\ll 1$. The radius R_A corresponds to the usual critical radius for a supersaturated domain, while R_B gives an estimate of the radius of the defect core. As stated before, the free energy in (11) grows with the size of the of the order of the separation between defects. In any case, the expressions for R_A and R_B are not modified significantly.

The effect of the ''elastic'' energy on the domain morphology is shown in Fig. 3, which presents the normalized domain size distribution function $f(R)$ at four different times: 50, 100, 200, and 500 (top to bottom). The white columns represent the size distribution function of charged domains, the gray columns correspond to neutral domains, and the black ones to the size distribution function of the total number of domains (i.e., the sum of charged and neutral domains). At a very early time most of the domains are formed in the proximity of defects, but as soon as $t=50$ the number of charged domains for a given radius is less than 50% of the total number of domains (i.e., the white column is shorter than the underlying gray column). This occurs for all radii except for very large ones. At $t=50$ the distributions of white, gray, and black columns are similar. As time evolves, the elastic energy enhances the growth of the charged domains, such that the location of the peak of the charged domain distribution shifts towards larger radii as compared to the location of the peak of the gray and black columns, i.e., neutral and total domain distributions. Note that at late times, $f(R)$ reflects the existence of R_B, as given by Eq. (12): a peak for $R<2$ develops at $t\approx 200$, persists and grows in relative height at later times.

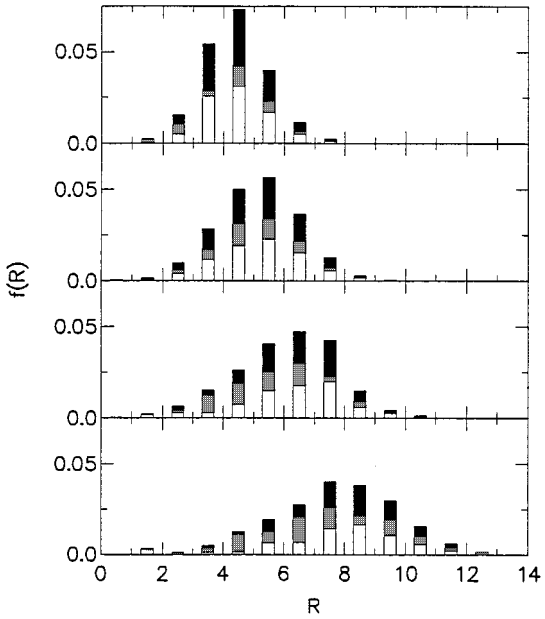

FIG. 3. Domain size distribution function $f(R)$ for the system shown in Fig. 1. From top to bottom times correspond to $t=50$, 100, 200, and 500. The white columns represent the size distribution function of charged domains, the underlying gray columns correspond to neutral domains, and the bottom black columns to the size distribution function of the total number of domains (i.e., the sum of charged and neutral domains).

B. Growth

As discussed previously, for $c_0>1/2$, the minority phase is ordered and the growth at late times resembles that of a model B system. Growth takes place via long-range diffusion, independent of the orientation of the order parameter inside each of the domains. In fact, the measured growth exponent $n\simeq 0.30$ is consistent with $n=1/3$, which is characteristic of the Lifshitz-Slyozov mechanism.

The situation is different for $c_0<1/2$. The differences between the vectorial model C, and that of a scalar model C become particularly clear in the limit of very small concentrations of the disordered phase. Here, the standard Lifshitz-Slyozov mechanism is modified by two effects: (i) the existence of another length scale R_B; and (ii) the long-range

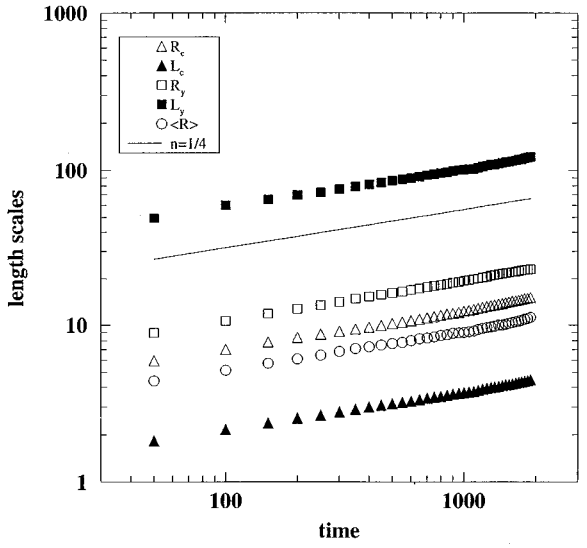

FIG. 4. Average length scales as function of time. For the concentration field, they are the first zero of the correlation function $\langle R_c \rangle$ (white triangle), the ''inverse perimeter'' L_c (black triangle), and the mean domain radius $\langle R \rangle$ (circle). For the order parameter, the lengths are $\langle R_y \rangle$ (white square), and the ''inverse perimeter'' L_y (black square).

attractive forces between domains. The presence of another length scale will not only modify the domain-size distribution function, but also the dynamics. Although R_B is generally smaller than the critical radius, domains of this size cannot just disappear by the usual curvature driven diffusion process, but have to coalesce with oppositely charged (or neutral) domains. Similarly, the long-range attraction between oppositely charged defects also favors a coalescence mechanism. Moreover, neutral domains are also attracted by charged domains, since the disordered concentration domains favor regions with large elastic energy. Thus coalescence mechanisms play a key role in the ordering.

Figure 4 shows a logarithmic plot of the different characteristic length versus time for $c_0=1/3$ and $l_y=1$. These lengths have been defined in Sec. II. For the concentration field, they are the first zero of the correlation function $\langle R_c \rangle$, the ''inverse perimeter'' L_c, and the mean domain radius $\langle R \rangle$. For the order parameter, the lengths are $\langle R_y \rangle$ and the ''inverse perimeter'' L_y. All these measured lengths are consistent with an $n=1/4$ exponent, at least over times less than ~ 1000. A qualitative explanation of this exponent is the following. Let S represent some characteristic distance between defects (e.g., $\langle R_y \rangle$, L_y, etc.). According to Eq. (10), the interaction energy in a neutral (zero total charge) system can be written as a sum of pair interactions: $E=-2\pi l_y^2 \Sigma_{ij} s_i s_j([r_{ij}/2r_c])$, with $r_c \ll r_{ij} \ll L$. The motion of the defects is described by a Langevin equation: $\partial \mathbf{r}_i/\partial t = -M(t)\nabla_i E$, where $M(t)$ is a mobility that may evolve in time. In terms of a characteristic length related to the distance between defects S, the Langevin equation can be written as $\partial S/\partial t \sim M(t) 1/S$. What is the functional form of the mobility $M(t)$? Every defect is trapped in a concentration domain, thus the defects can only annihilate by coalescence of domains. This means that the mobility of defects is proportional to the mobility of the concentration domains, which can only move through diffusion. Since the time evolution of the concentration is described by a diffusion equation without hydrodynamics, the mobility of a domain of radius R is inversely proportional to its volume. Thus $M(t) \sim 1/R(t)^2$ in 2d. As shown in Fig. 4, the characteristic concentration length scale R is proportional to S. Therefore, the defect Langevin equation becomes $\partial S/\partial t \sim 1/S^3$, which implies $S \sim t^{1/4}$. There are also charged domains that coalesce with neutral domains. For the case of small domains, the part of the energy that considers the attraction between a charged domain and a neutral domain of radius R_n separated by a distance S is $E_n \propto -R_n^2/S^2$ so that $\partial S/\partial t \sim (1/R_n^2)\partial E_n/\partial S$. This again gives $S \sim t^{1/4}$, subject to possible logarithmic corrections.

The results for $l_y=4$ are consistent with those in Fig. 4. At any given time the numbers of droplets and of defects in the $l_y=4$ systems are fewer than that in the $l_y=1$ systems: the energy cost produced by the term $l_y^2|\nabla \mathbf{y}|^2$ in the free-energy favors, for larger l_y's a higher rate of coalescence of droplets and a faster elimination of defects.

Although our results are clearly consistent with an $n=1/4$ growth exponent, at late times the system might cross over to $n=1/3$ Lifshitz-Slyozov type growth. Over most of the time scales probed by our simulations, the dynamics is dominated by the coalescence and annihilation of defects. However, long-range diffusion, which is always acting, can be expected to play more and more of a role as the number of defects present in the system becomes less and less. At some point, the concentration of defects becomes negligible and the dynamics will then cross over. While we have not been able to probe this time regime effectively with the computer resources currently available to us, there is some evidence indicating a possible crossover. For $t \approx 1500$ and higher, the effective exponent increases from $n=1/4$ to $n \approx 0.30$, which is not inconsistent with Lifshitz-Slyozov type of growth.

IV. SUMMARY

In this paper we have investigated the dynamics of a model C system characterized by a two-component vectorial order parameter and a coupled concentration variable, following a temperature quench from its high-temperature disordered state into the order-disorder coexistence region. Because of the vectorial nature of the order parameter, the existence of order-order interfaces is precluded. Rather, vortices with integral charge are generated by the order parameter field. The specific domain morphology obtained is dependent upon the mean concentration c_0.

If $c_0 > 1/2$, the minority phase is the ordered phase. Here, isolated droplets, inside which complete order of the vectorial field is achieved, form. The presence of the vectorial nature of the order parameter manifests itself chiefly in the shape of the domains. Initially these tend to be elongated, bent and sometimes branched. At late times they assume a more circular shape, characteristic of model C and B systems. Growth of the domains takes place via long-range diffusion with a measured growth exponent consistent with an $n=1/3$ exponent.

If $c_0 < 1/2$, the minority phase is the disordered one. The domains of the disordered phase are now droplets, where the order parameter has $|\mathbf{y}|=0$. There is no elastic energy inside

these droplets. Since the regions close to a vortex are characterized by large elastic energy densities, it is energetically favorable for vortices to center themselves on the disordered domains. As a consequence, the growth is dominated by the coalescence and annihilation of defects. Both the attraction between oppositely charged domains, and the attraction between neutral and charged domains, contribute to this effect. Droplets upon which the defect cores are centered contribute to this effect. The coalescence mechanism is characterized by $n \sim 1/4$, and possibly may crossover to $n \sim 1/3$ at very late times when the number of charged domains becomes negligible and the dominant mechanism of growth reverts to that of long-range diffusion.

ACKNOWLEDGMENTS

We thank the following agencies for financial support: A.M.S acknowledges Grant No. PB94-0005-C02 DGICyT, Spain; C.M.R. acknowledges the donors of the American Chemical Society for Grant No. 27092-G9. We also thank the North Carolina Supercomputing Center for computer time.

[1] *Dynamics of Ordering Processes in Condensed Matter*, edited by S. Komura and H. Furukawa (Plenum, New York, 1988).
[2] K. Kawasaki, Ann. Phys. (N.Y.) **154**, 319 (1984).
[3] A. J. Bray, Adv. Phys. **43**, 357 (1994).
[4] P.C. Hohenberg and B.I. Halperin, Rev. Mod. Phys. **47**, 435 (1977).
[5] S.M. Allen and J.W. Cahn, Acta Metall. **27**, 1085 (1979); K. Kawasaki, M.C. Yalabik, and J.D. Gunton, Phys. Rev. A **17**, 455 (1978).
[6] I.M. Lifshitz and V.V. Slyozov, J. Phys. Chem. Solids **19**, 35 (1961).
[7] A.J. Bradley and A.H. Jay, Proc. R. Soc. London Ser. A **136**, 210 (1932).
[8] A.M. Somoza and C. Sagui, Phys. Rev. E **53**, 5101 (1996).
[9] A.P.Y. Wong, P. Wiltzius, R.G. Larson, and B. Yurke, Phys. Rev. E **47**, 2683 (1993).
[10] C.D. Muzny and N.A. Clark, Phys. Rev. Lett. **68**, 804 (1992).
[11] B. Morin, K. Elder, M. Sutton, and M. Grant, Phys. Rev. Lett. **75**, 2156 (1995).
[12] N.D. Mermin, Rev. Mod. Phys. **51**, 591 (1979).
[13] J.M. Kosterlitz and D.J. Thouless, J. Phys. C **6**, 1181 (1973).
[14] A.N. Pargellis, S. Green, and B. Yurke, Phys. Rev. E **49**, 4250 (1994).
[15] R. Loft and T.A. DeGrand, Phys. Rev. B **35**, 8528 (1987).
[16] M. Mondello and N. Goldenfeld, Phys. Rev. A **42**, 5865 (1990).
[17] H. Toyoki, Phys. Rev. A **42**, 911 (1990).
[18] B. Yurke, A.N. Pargellis, T. Kovacs, and D.A. Huse, Phys. Rev. E **47**, 1525 (1993).
[19] E.D. Siggia and D.R. Nelson, Phys. Rev. B **15**, 1427 (1977); P.C. Hohenberg and D.R. Nelson, *ibid.* **20**, 2665 (1979).
[20] Simulations on discrete lattices may suffer from ''lattice friction''; i.e., a small energy barrier needs to be overcome before an isolated defect can be translated. In many simulations, a weak noise term will ensure that the barrier is overcome. For our model, we do not expect lattice friction to be a problem. Lattice friction disappears in the continuous limit, i.e., when the mesh size $dx \to 0$. We have taken care to consider a relatively small dx, so that the defect core is always larger than dx. For $l_y = 1$ the core occupies between five and ten lattice points, and for increasing l_y the defect cores becomes much larger. There is also one more important reason that eliminates the problem of lattice friction in our simulations. The problem of lattice friction arises mainly when the length of the spin is fixed in every point of the system. For instance, consider a Monte Carlo simulation for the XY model where every spin is of length unity. There, the size of the defect core is effectively zero and its localization in the lattice may be important. However, in our simulations the modulus of the vectorial order parameter varies and it approaches zero in the defect core. This implies that the energy barrier becomes negligible.